Hydrogen Evolution Reaction Evaluation in Aqueous Solutions Containing H_2S at Different Pressures

Pedro R. P. Viana[a], Flávio V. V. de Souza[a], Oswaldo E. Barcia[a], Oscar R. Mattos[a]

Abstract

H_2S corrosion has been a known problem in oil/gas production and transport since 1940, which was enhanced after the discovery of huge oil and gas reserves in the pre-salt layer. The presence of H_2S in free water may cause severe corrosion problems in oil and gas pipes and is mainly influenced by temperature, H_2S content, fluid velocity, oil composition, pH and steel surface conditions. This work addresses the hydrogen evolution reaction (HER) occurring on platinum in an aqueous solution containing dissolved H_2S at several pressures. A new setup that uses a low inertia rotating disc electrode (RDE) adapted in an autoclave is proposed. This setup allows obtaining polarizations curves and electro-hydrodynamic (EHD) impedances, the latter for the first time in pressured conditions.

Keywords: Hydrogen Evolution Reaction, H_2S, Rotating Disc Electrode. EHD Impedance.

Introduction

H_2S corrosion has been a known problem in oil/gas production and transport since 1940, which was enhanced after the discovery of huge oil and gas reserves in the pre-salt layer, as mentioned by Costa (1) and Obuka (2). The presence of H_2S and free water may cause severe corrosion problems in oil and gas pipes and is mainly influenced by temperature, H_2S content, fluid velocity, oil composition, pH and steel surface conditions. The corrosion rate can change considerably due to a small variation of these parameters and may be strongly reduced if mackinawite ($Fe_{1+x}S$) and/or pyrite (FeS_2) precipitates on the steel surface, forming a dense and compact protective film, occurring easier at high temperature and pH, according to Obuka (2). However, localized corrosion with extremely high corrosion rates may occur when this corrosion product does not provide sufficient protection. Although it has been studied in details by Smith (3) and Nešić (4), the H_2S steel corrosion mechanism is not yet totally understood. Only recently, new ideas were proposed by Bolmer (5), Galvan-Martinez (6) and Kittel (7) about the cathodic reduction and about the anodic role of H_2S in the global corrosion process. The major limitation of the proposed mechanisms until now is the experimental approach used, in general restricted to steady state techniques. Indeed, although very important, adapting the transient techniques to an autoclave and working at high pressure is not an easy task. Thus, the objective of this study is to present new results using a new setup that allows working with a low inertia rotating disk electrode (RDE) adapted in an autoclave. This setup allows obtaining polarization curves and electro-hydrodynamic (EHD)

[a] Master-Ph.D. Student, Chemist – Federal University of Rio de Janeiro
[a] Master-Researcher, Chemist – Federal University of Rio de Janeiro
[a] Ph.D.-Professor – Federal University of Rio de Janeiro
[a] Ph.D.-Professor – Federal University of Rio de Janeiro

impedance, the latter for the first time in pressurized conditions. Indeed, although very useful for problems related to mass transport in the electrochemical field, EHD impedance has been used by few research groups, such as Remita (8) and Deslouis (9), but never at high pressures. The present work deals with hydrogen evolution reaction (HER) in aqueous solutions containing H_2S at different pressures.

Methodology

The Figure 1 presents the new setup used to work at high pressure with a RDE. The RDE was adapted to a miniclever magnetic stirrer head from Premex. This magnetic coupling can work up to 6 MPa and 200 °C of temperature. The setup was assembled in a 1L Hastelloy autoclave and it was coupled with a low inertia motor allowing EHD impedance measurements.

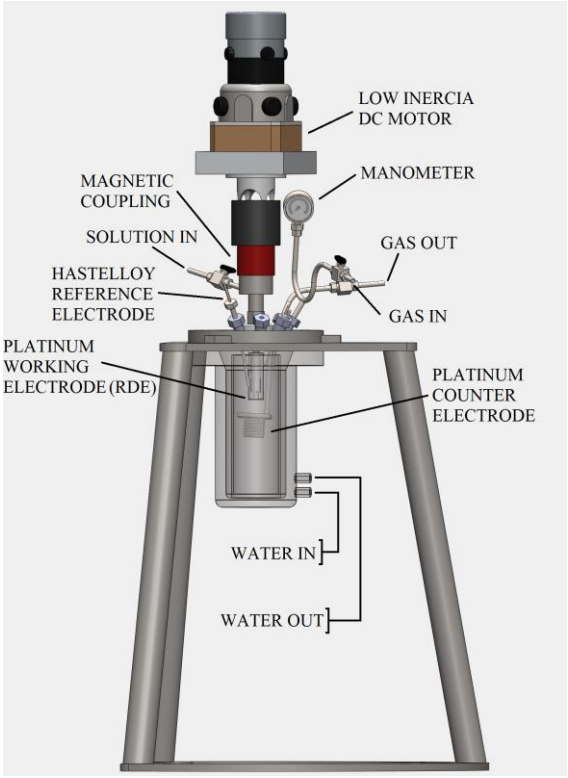

Figure 1 – Schematic test setup

All experiments in this work were performed using 0.01 mol/L K_2SO_4 solution as supporting electrolyte. Analytical grade reagents and double distilled water were used for preparing the solution. A 0.126 cm^2 platinum RDE embedded in polyetheretherketone (PEEK), abraded with #1500 grit paper, was used as working electrode (WE). A large platinum grid was used as counter electrode and a Hastelloy rod as reference (E = + 0,030 mV SSE). This value was constant during all long the experience time. All potentials, although measured versus Hastelloy, were later referred to saturated sulfate electrode (SSE).
Electrochemical measurements were carried out at room temperature (25 °C ± 1 °C) using a Reference 600 Potentiostat from Gamry monitored by a personal computer. Potential scans were performed from the open circuit potential to around -1.4 V (SSE) at a rate of 1.00 mV/s to obtain polarization curves in the hydrogen evolution domain. All potential scans were done in triplicate in 1% H_2S/99% N_2 saturated conditions and in N_2 purged conditions (oxygen

free). Gas saturation was obtained by purging the test solutions with 1% H_2S/99% N_2 or pure N_2 during at least 2 h. The pH of the N_2 purged solutions was adjusted with H_2SO_4 to pH = 4.00. H_2S tests were carried out at 0.1, 0.5, 1.0, 1.5, 2.0 and 3.0 MPa. N_2 tests were conducted at 0.1 and 3.0 MPa. All pH measurements were performed using a Thermo Scientific Orion Dual Star pH meter. For 0.1 MPa tests, a slight gas overpressure was maintained inside the autoclave to avoid oxygen contamination. According to simulations performed using OLI commercial software, pH and other parameters were calculated and are presented in Table 1.

Table 1 – Parameters calculated by OLI software

1%H_2S/N_2 total pressure (MPa)	[H_2S] in liquid phase (mol/L)	[HS^-] in liquid phase (mol/L)	[S^{2-}] in liquid phase (mol/L)	[H^+] in liquid phase (mol/L)	Absolute Viscosity (mPa.s)	Relative Viscosity (mPa.s / mPa.s H_2O)	pH
0.1	$9.36.10^{-4}$	$1.40.10^{-5}$	$3.82.10^{-13}$	$9.66.10^{-6}$	0.8936	1.00324	5.088
0.5	$4.30.10^{-3}$	$2.99.10^{-5}$	$3.84.10^{-13}$	$2.07.10^{-5}$	0.8936	1.00324	4.756
1.0	$7.64.10^{-3}$	$3.99.10^{-5}$	$3.85.10^{-13}$	$2.77.10^{-5}$	0.8936	1.00324	4.630
1.5	$1.03.10^{-2}$	$4.64.10^{-5}$	$3.87.10^{-13}$	$3.22.10^{-5}$	0.8936	1.00324	4.565
2.0	$1.24.10^{-2}$	$5.11.10^{-5}$	$3.89.10^{-13}$	$3.55.10^{-5}$	0.8936	1.00324	4.522
3.0	$1.57.10^{-2}$	$5.75.10^{-5}$	$3.93.10^{-13}$	$4.00.10^{-5}$	0.8936	1.00324	4.470

Potentiostatic EHD impedances were obtained by linear sinusoidal modulation of the angular velocity of the disk, which was rotated by a low inertia dc *dc* motor. The setup was constituted of an Ohmnimetra potentiostat and a Solartron frequency response analyzer (FRA Solartron 1250) controlled by a personal computer. EHD measurements were performed from 70 Hz up to 10 mHz with an increment of 7 points/decade at the same temperature and pressures of the potentiodynamic experiments aforementioned.

Results and discussion

Before starting the experimental tests, it was necessary to certify the experimental setup used. The setup shown in Figure 1 was new and had to be verified using a classical system involving a well-known electrochemical reaction, carried out using a solution of potassium ferricyanide-ferrocyanide 0.005 mol/L with 1.00 mol/L KCl as supporting electrolyte and at pressures of 0.1 and 3.0 MPa of pure N_2. EHD impedance results were compared with theoretical curves obtained by Tribollet and Newman (10). The results are shown in Figure 2.

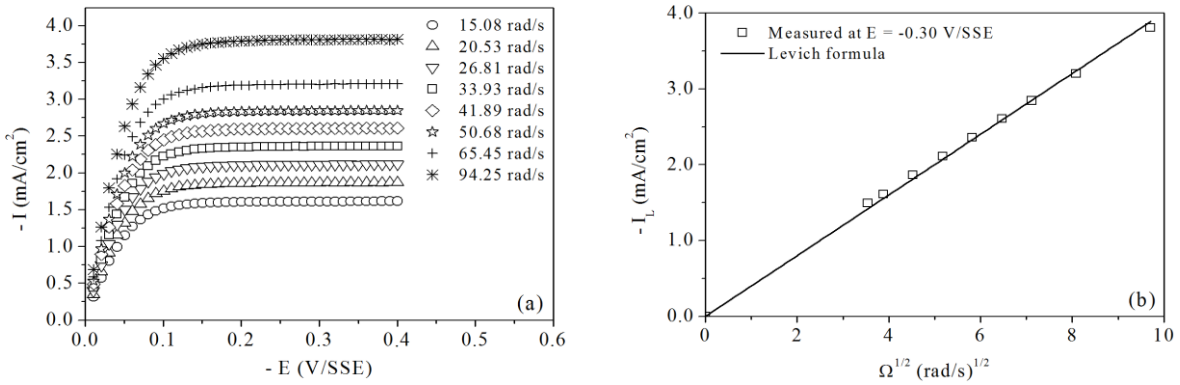

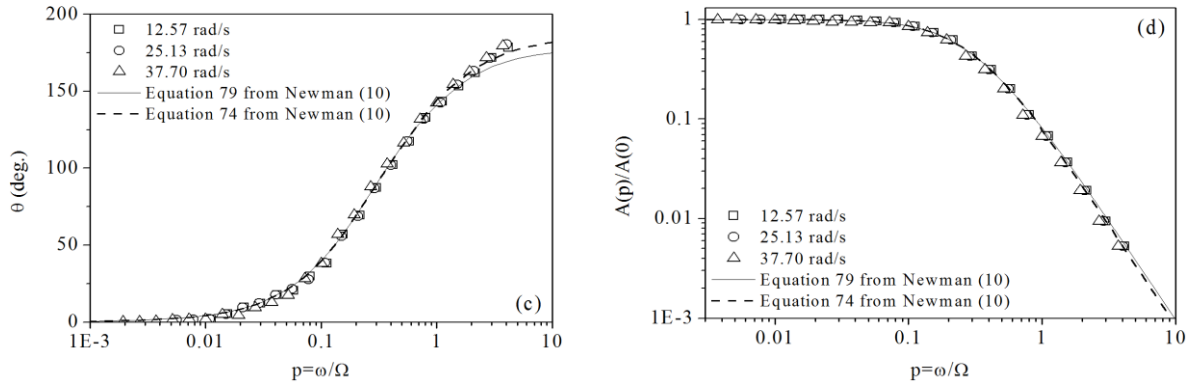

Figure 2 – Classical results for the reduction of $Fe(CN)_6^{3-}$ to $Fe(CN)_6^{4-}$ in 1 mol/L KCl, attesting the new experimental setup for 0.1 or 3.0 MPa of N_2. (a) Polarization curves, (b) Levich plot, (c) phase shift vs. dimensionless frequency and (d) normalized amplitude vs. dimensionless frequency. Theoretical data calculated using F = 96485.33 C/mol, C(∞) = 0.005 mol/L, Sc = 1200, D = 0.765.10^{-5} cm^2/s, ν = 0.0094 cm^2/s

As expected, the results were the same at high and atmospheric pressures and so, only the 0.1 MPa results are presented. Figures 2(a) and 2(b) show the stationary results and Figures 2(c) and 2(d) present EHD impedance results. In both cases, the results obtained were consistent with literature data and the theoretical curves fitted the experimental results.

After certifying that the experimental setup is calibrated, it was used a system using a neutral gas, such as N_2. The Figure 3 presents the cathodic polarization curves obtained in 0.01 mol/L K_2SO_4 at two N_2 pressures and pH = 4.00.

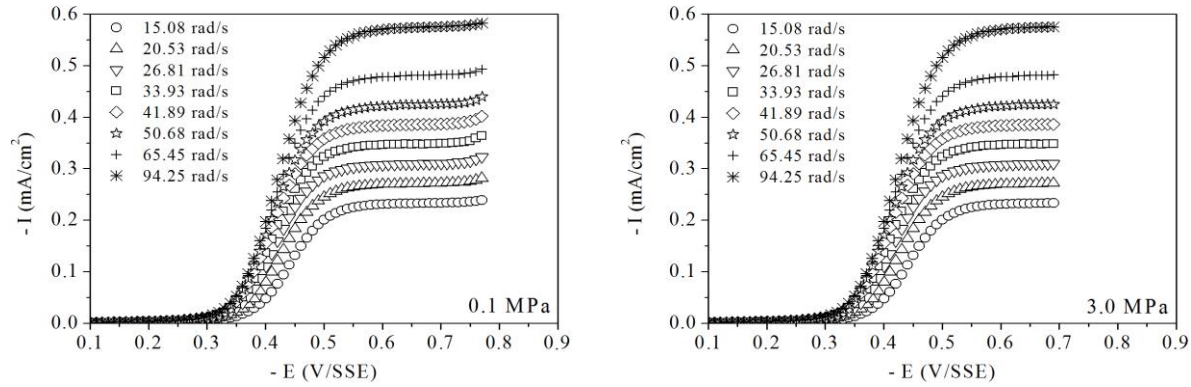

Figure 3 – Polarization curves obtained using 0.01 mol/L K_2SO_4 and two N_2 pressures

As it can be seen, the pressure does not influence the results. At very small polarization, the curves show a region fully controlled by charge transfer. With increasing polarization a second region appears where the electrochemical process is controlled by both mass transport and charge transfer. Finally, at high polarization a current plateau is detected. In this third region, the value of current density (I_L) is entirely controlled by mass transport.

The Figure 4(a) shows the plot of I_L vs. $\Omega^{1/2}$, where Ω is the disk rotation speed. A linear behavior passing through the origin is seen while the Figure 4(b) shows the Koutecký-Levich plots and, as expected, a linear behavior passing through the origin is also observed.

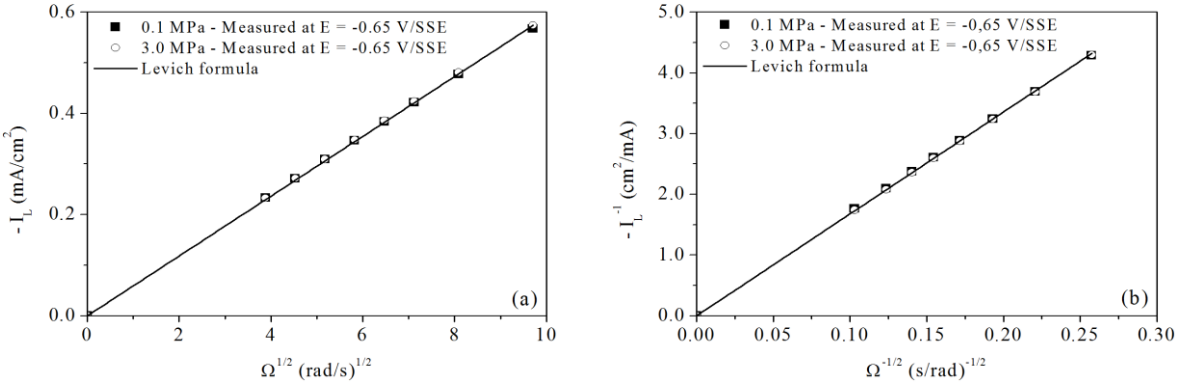

Figure 4 – Hydrogen cathodic current limit plots for 0.1 and 3.0 MPa of N_2 (pH = 4.00). Theoretical data calculated using F = 96485.33 C/mol, C(∞) = $1.39.10^{-4}$ mol/L, D = $9.3.10^{-5}$ cm^2/s, ν = 0.01 cm^2/s

Total pressure did not influence the kinetics of hydrogen cathodic reaction and the theoretical equations were used to fit the experimental results.

In H_2S pressured system, the Figure 5 presents the polarization curves at different H_2S pressures.

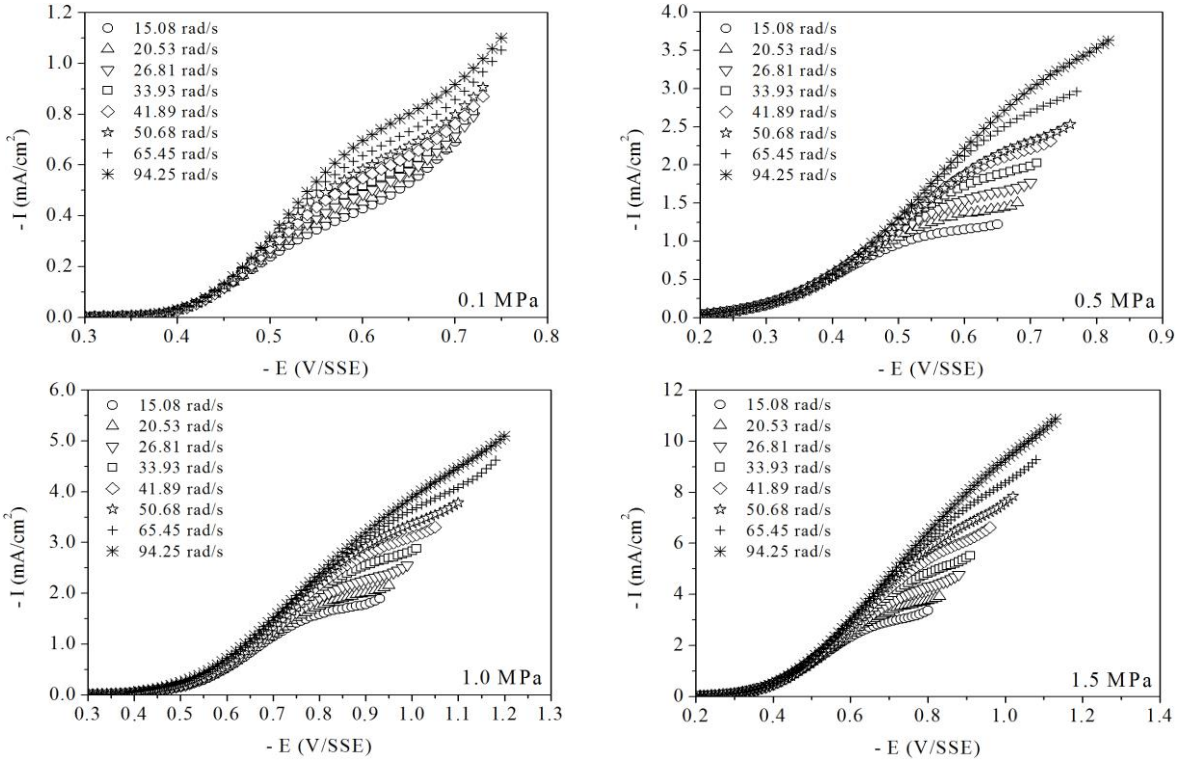

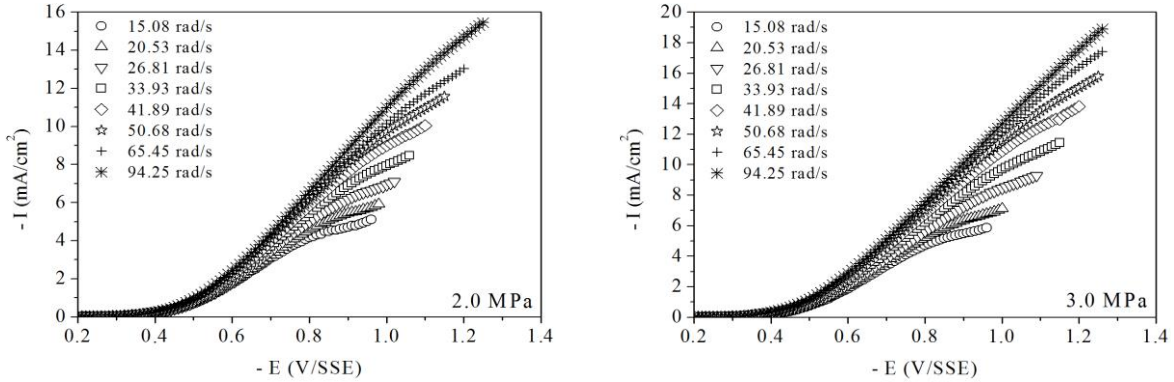

Figure 5 – Polarization curves for 0.01 mol/L K_2SO_4 in different H_2S pressures

Analyzing the Figure 5, it is evident that increasing pressure significantly increases the current, showing the influence of H_2S pressure on the electrochemical system. However, the behavior observed in these curves are different that observed in Figure 3, because it is not possible to distinguish clearly a region entirely controlled by mass transport. For the H_2S pressured system, observes that with increasing pressure there are clearly regions controlled by charge transfer and mixed control, but for rotations between 15.08 and 33.93 rad/s, there is no clear distinction of a current plateau, can be described as a "pseudo plateau", that shows an exclusive control by mass transfer, so that for high values of cathodic overpotentials, the water reduction reaction is also observed. For rotations above 41.89 rad/s, it is not possible even to distinguish the water reduction reaction, since the region by charge transfer becomes preponderant. According with Tribollet (11), H_2S dissociation it is extremely fast, so that is possible to suggest that H^+ diffusion from bulk solution to the electrode surface is high. In the work of Nordsveen (12), it was estimated that the reaction rate coefficient of H^+ formation, in H_2S medium, is equal to 10^4 s^{-1}.

Figures 6(a) and 6(b) show the plots of I_L vs. $\Omega^{1/2}$ and I_L^{-1} vs. $\Omega^{-1/2}$ referring to the plateau currents seen in Figure 5 between 15.08 and 41.89 rad/s.

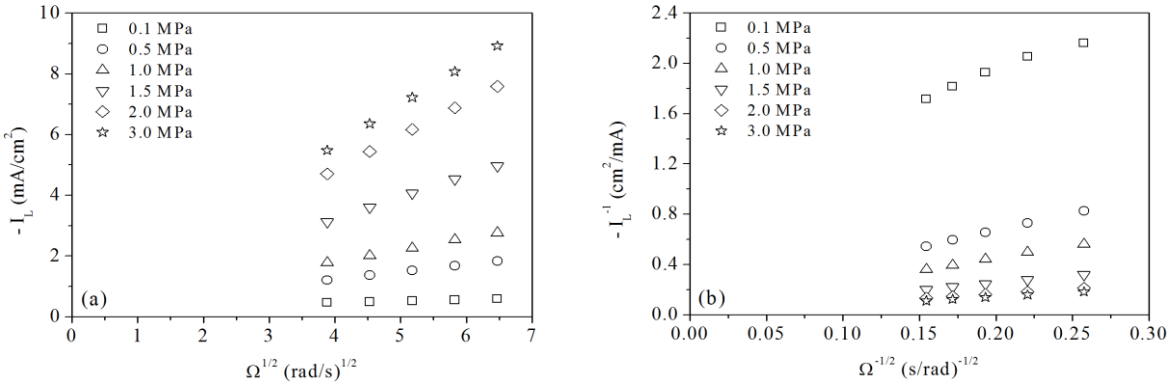

Figure 6 – Levich plots for 0.01 mol/L K_2SO_4 + 1% H_2S/99% N_2

Both curves could be considered as having a linear behavior not passing through the origin. $I_L = I_0 + A\Omega^{1/2}$ for Figure 6(a) or $I_L^{-1} = I_\infty^{-1} + B\Omega^{-1/2}$ for Figure 6(b) and the parameters I_0 and A as well as I_∞ and B can be obtained by fitting. However, actually, it is evident that Figures 6(a) and 6(b) cannot simultaneously present a linear behavior. In the literature, Schmitt and Rothmann (13) considered I_L linear with $\Omega^{1/2}$ and interpreted $A\Omega^{1/2}$ as the transport of the electroactive species and, I_0, which is independent of diffusion, as being due to a chemical

reaction in the bulk of the solution. However, the Koutecký-Levich equation, or I_L^{-1} linear with $\Omega^{-1/2}$, was also proposed for the case of a chemical-electrochemical (CE) mechanism.
EHD impedance results for several H_2S pressures and for 0.1 MPa of N_2 are presented in Figures 7, 8 and 9.

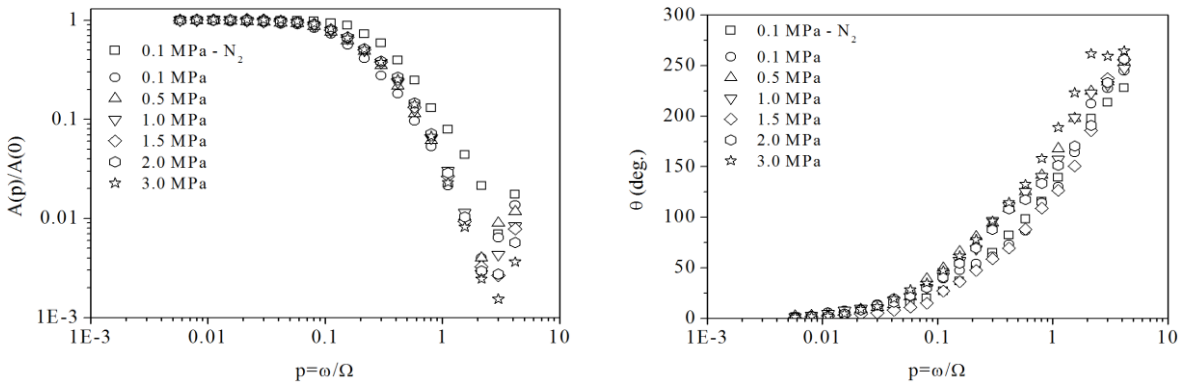

Figure 7 – Comparison between experimental data of several pressures. Normalized amplitude vs. dimensionless frequency (left) and phase angle vs. dimensionless frequency (right) for 120 rpm

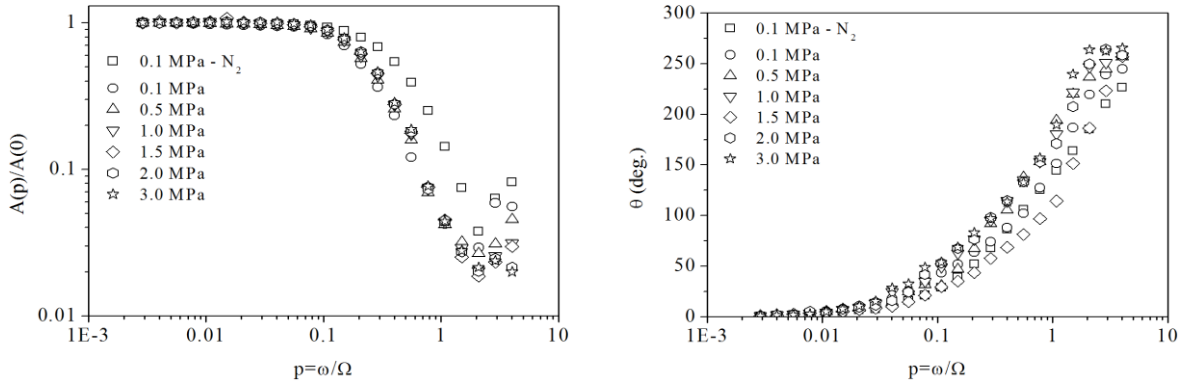

Figure 8 – Comparison between experimental data of several pressures. Normalized amplitude vs. dimensionless frequency (left) and phase angle vs. dimensionless frequency (right) for 240 rpm

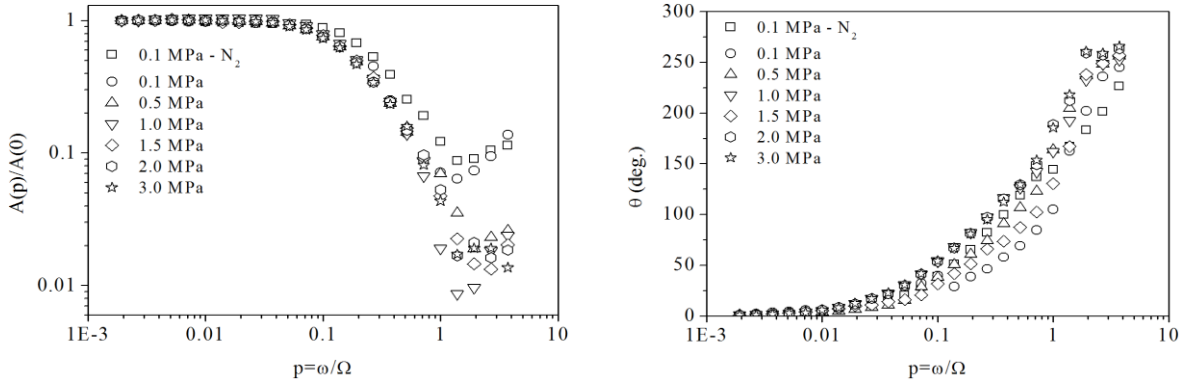

Figure 9 – Comparison between experimental data of several pressures. Normalized amplitude vs. dimensionless frequency (left) and phase angle vs. dimensionless frequency (right) for 360 rpm

Qualitatively the same result was obtained in the presence of N_2 and H_2S, although in the presence of the latter, the curves were translated for small values of p, the dimensionless frequency. Essentially, EHD impedance measures the fluctuation of the kinetic parameters

associated with hydrodynamic and mass transport; i.e., parameters A and B. The presence of two time constants in Figures 7, 8 and 9 when H_2S is present can be associated with mass transport (parameters A and B in the above equations) coupled with a chemical reaction (parameter I_0), according to Tribollet (9) and Treimer (14). However, only an analytical model can define the specific coupling process. In this sense, the model suggested by Remita (8) proposing a buffer effect for H_2S could be envisaged. Nevertheless, it would be necessary to introduce the pressure dependence in this model and better describe H_2S pressure dependence in the chemical-electrochemical coupling reactions.

Conclusions

A new experimental setup was validated for working in a high pressure system adapted to obtain steady state and transient results. The setup was used to study hydrogen reaction in the presence of H_2S at different pressures. Non linear behavior was found for I_L vs. $\Omega^{1/2}$ and I_L^{-1} vs. $\Omega^{-1/2}$. EHD impedances results were compatible with a chemical-electrochemical process and the development of an analytical model for different H_2S pressures is still needed.

Referências bibliográficas

(1) COSTA, T. Corrida para o mar, **COPPE/UFRJ**, Rio de Janeiro, 14 dez 2014. Available in: http://www.coppe.ufrj.br/pdf_revista/coppe_pre-sal.pdf

(2) OBUKA, N. S. P., OKOLI, N. C., IKWU, G. R. O., CHUKWUMUANYA, E. O. Review of corrosion kinetics and thermodynamics of CO_2 and H_2S corrosion effects and associated prediction/evaluation on oil and gas pipeline system, **International Journal of Scientific Technology and Research**, India, v. 1, n. 156, p. 156-162, May 2012.

(3) SMITH, S. N., JOOSTEN, M. W., Corrosion of carbon steel by H_2S in CO_2 containing oilfield environment, **CORROSION/2006**, paper no. 06115, Houston, TX: NACE International, March 2006.

(4) NEŠIĆ, S., POSTLETHWAITE, J., OLSEN, S. An electrochemical model for prediction of corrosion of mild steel in aqueous carbon dioxide solutions, **Corrosion**, Houston, v. 52, p. 280-294, 1996.

(5) BOLMER, P. W. Polarization of iron in H_2S-NaHS buffers, **Corrosion**, Houston, v. 21, n. 3, p. 69-75, March 1965.

(6) GALVAN-MARTINEZ, R., MENDOZA-FLORES, J., DURAN-ROMERO, R., GENESCA, J. Effect of turbulent flow on the anodic and cathodic kinetics of API X52 steel corrosion in H_2S containing solutions. A rotating cylinder electrode study, **Materials and Corrosion**, Weinhein, v. 58, n. 7, p. 514-521, July 2007.

(7) KITTEL, J., ROPITAL, F., GROSJEAN, F., SUTTER, E. M. M., TRIBOLLET, B. Corrosion mechanisms in aqueous solutions containing dissolved H_2S. Part 1: Characterisation of H_2S reduction on a 316L rotating disc electrode, **Corrosion Science**, Oxford, v. 66, p. 324-329, January 2013.

(8) REMITA, E., TRIBOLLET, B., SUTTER, E., VIVIER V., ROPITAL, F., KITTEL, J. Hydrogen evolution in aqueous solutions containing dissolved CO2: Quantitative contribution of the buffering effect, **Corrosion Science**, Oxford, v. 50, p. 1433-1440, 2008.

(9) DESLOUIS, C., TRIBOLLET, B. Flow modulation technique and EHD impedance: A tool for electrode process and hydrodynamics studies, **Electrochimica Acta**, Great Britain, v. 35, n. 10, p. 1637-1648, April 1990.

(10) TRIBOLLET, B., NEWMAN, J. The modulated flow at a rotating disk electrode, **Journal of Electrochemical Society**, New Jersey, v. 130, n. 10, p. 2016-2026, October 1983.

(11) TRIBOLLET, B., KITTEL. J., MEROUFEL, A., GROSJEAN, F., SUTTER, E. M. M. Corrosion mechanisms in aqueous solutions containing dissolved H_2S. Part 2: Model of the cathodic reactions on a 316L stainless steel rotating disc electrode, **Electrochimica Acta**, Great Britain, v. 124, n. 1, p. 46-51, January 2014.

(12) NORDSVEEN, M., NEŠIĆ, S., NYBORG, R., STANGELAND, A. A mechanistic model for carbon dioxide corrosion on mild steel in the presence of protective iron carbonate films – Part 1: Theory and verification, **Corrosion**, Houston, v. 59, n. 5, p. 443-456, May 2003.

(13) SCHMITT, G., ROTHMANN, B. Studies on the corrosion mechanism of unalloyed steel in oxygen-free carbon dioxide solutions part I. Kinetics of the liberation of hydrogen, **Werkstoffe und Korrosion**, Weinhein, v. 28, n. 12, p. 816-822, December 1977.

(14) TREIMER, S., TANG, A., JOHNSON, D. C. A consideration of the application of Koutecký-Levich plots in the diagnoses of charge-transfer mechanisms at rotated disk electrodes, **Electroanalysis**, Weinhein, v. 14, n. 3, p. 165-171, February 2002.